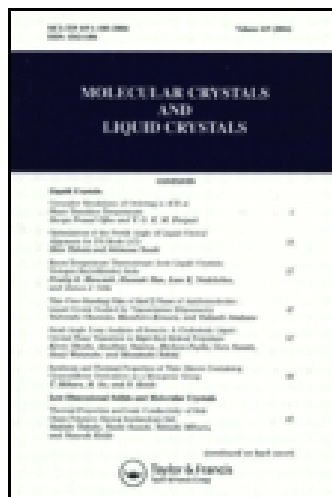


This article was downloaded by: [University of Connecticut]  
On: 08 October 2014, At: 14:43  
Publisher: Taylor & Francis  
Informa Ltd Registered in England and Wales Registered Number: 1072954  
Registered office: Mortimer House, 37-41 Mortimer Street, London W1T 3JH,  
UK



## Molecular Crystals and Liquid Crystals

Publication details, including instructions for authors and subscription information:

<http://www.tandfonline.com/loi/gmcl20>

### Naphthalene Core-Based Mesogens with Terminal Halogen Substituents: Synthesis and Mesomorphic Behavior

B. T. Thaker <sup>a</sup> & P. K. Tandel <sup>a</sup>

<sup>a</sup> Department of Chemistry , South Gujarat University , Surat, India

Published online: 17 Oct 2011.

To cite this article: B. T. Thaker & P. K. Tandel (2006) Naphthalene Core-Based Mesogens with Terminal Halogen Substituents: Synthesis and Mesomorphic Behavior, *Molecular Crystals and Liquid Crystals*, 451:1, 127-138, DOI: [10.1080/15421400600580154](https://doi.org/10.1080/15421400600580154)

To link to this article: <http://dx.doi.org/10.1080/15421400600580154>

PLEASE SCROLL DOWN FOR ARTICLE

Taylor & Francis makes every effort to ensure the accuracy of all the information (the "Content") contained in the publications on our platform. However, Taylor & Francis, our agents, and our licensors make no representations or warranties whatsoever as to the accuracy, completeness, or suitability for any purpose of the Content. Any opinions and views expressed in this publication are the opinions and views of the authors, and are not the views of or endorsed by Taylor & Francis. The accuracy of the Content should not be relied upon and should be independently verified with primary sources of information. Taylor and Francis shall not be liable for any losses, actions, claims, proceedings, demands, costs, expenses, damages, and other liabilities whatsoever or howsoever caused arising directly or

indirectly in connection with, in relation to or arising out of the use of the Content.

This article may be used for research, teaching, and private study purposes. Any substantial or systematic reproduction, redistribution, reselling, loan, sub-licensing, systematic supply, or distribution in any form to anyone is expressly forbidden. Terms & Conditions of access and use can be found at <http://www.tandfonline.com/page/terms-and-conditions>

## Naphthalene Core-Based Mesogens with Terminal Halogen Substituents: Synthesis and Mesomorphic Behavior

**B. T. Thaker**  
**P. K. Tandel**

Department of Chemistry, South Gujarat University, Surat, India

*We report three series of naphthalene core-based mesogens obtained by varying two different terminal substituents. The flexibility in these systems is provided by attaching a straight alkoxy chain at the one end, while a halogen terminal substituent accounts for the polarity. To understand the structure–property relation, alkoxy tails ( $C_1$  to  $C_8$ ,  $C_{10}$ ,  $C_{12}$ ,  $C_{14}$ ,  $C_{16}$ , and  $C_{18}$ ) as well as halogen atoms (F, Cl, and Br) have been varied. The molecular structures of these mesogens have been confirmed by spectroscopic and elemental analyses, whereas their thermal behavior was evaluated mainly by polarizing optical microscopic observations. The study shows that, in general, all the compounds display nematic and/or smectic A mesophases. In all three series of compounds, the lower and middle homologues exhibit the nematic phase only and higher homologues also display the smectic A phase. These compounds follow the general trend that with the increase in the length of alkoxy tail, the nematic to isotropic phase transition temperature decreases, which is reminiscent of a large number of reported homologues series. The transition temperatures of the compounds with fluoro substituents are significantly lower when compared to the materials with chloro or bromo substitutions.*

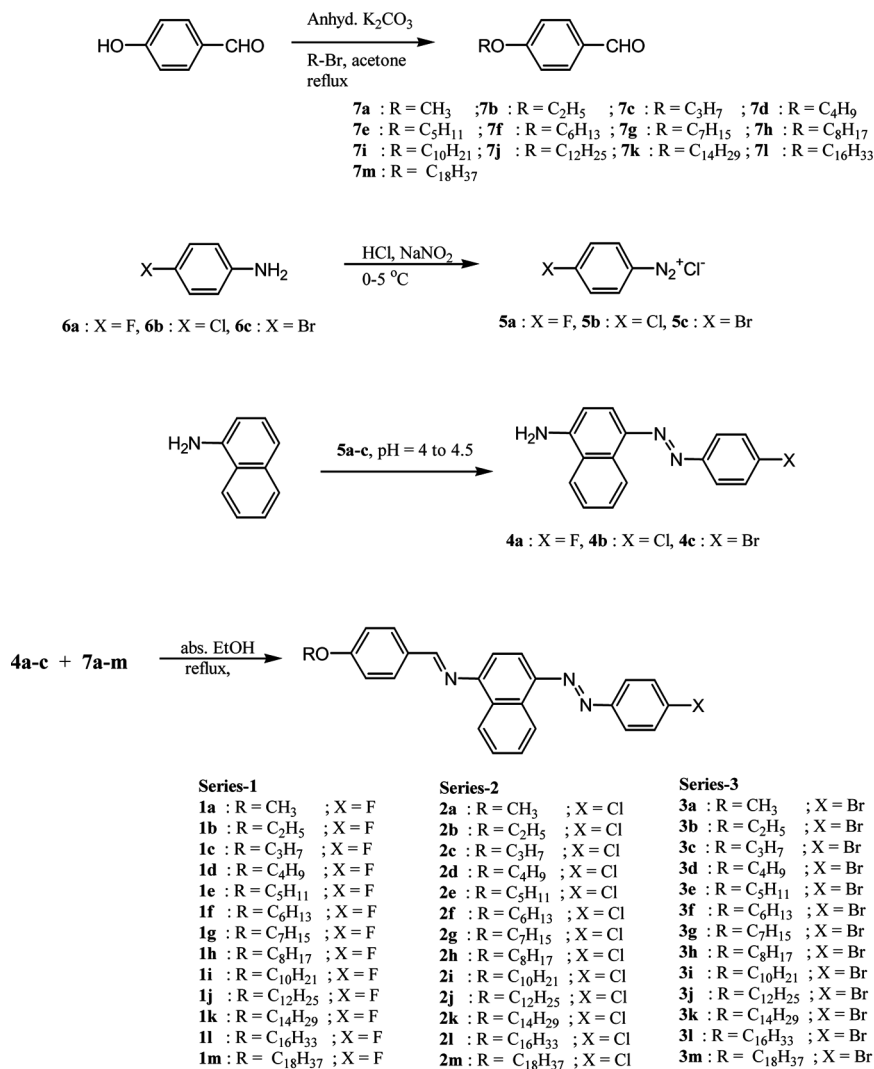
**Keywords:** azomethine; mesogens; naphthalene; nematic and smectic

### 1. INTRODUCTION

Thermotropic liquid crystals are of great technological importance [1]. Schiff base compounds are synthesized in large numbers as these compounds exhibit nematic and smectic mesophases [2,3]. The interest in synthesis and structural investigations of liquid crystalline Schiff bases with azo-groups in the mesogenic units has considerably increased because of their potential application in the field of

Address correspondence to B. T. Thaker, Department of Chemistry, South Gujarat University, Surat 395 007, India. E-mail: btthaker1@yahoo.co.in

nonlinear optics, in optical storage devices, and in electrooptical displays. The photoresponsive azobenzene group appears particularly interesting because irradiation can induce the trans-cis isomerization of the photo chromic group, including a local phase transition. Mesomorphic properties of some homologous series of Schiff bases



SCHEME 1

containing a naphthalene core are well known. Wiegand prepared and studied liquid crystalline properties of anisilidene amino naphthalenes [4,5]. Dave *et al.* reported the mesomorphic behavior of a homologous series obtained by condensing 4-*n*-alkoxy-1-naphthaldehydes with benzidine [6]; *p*-phenylene diamine [7], and *p*-amino benzoic acid [8]. Arora and Ferguson studied a benzylidene Schiff base series containing an azo group [9].

In continuation of our investigations on naphthalene based rod-like liquid crystals, it was thought that the introduction of an azo group in a naphthylidene series with halogens and alkoxy tails as terminal substituents could help in further understanding the underlying structure–property relation. Here we report three series of mesogens, namely, 4-[4'-*n*-alkoxybenzylidene amino]naphthalene-1-(4''-halo-1-azobenzene) in which alkoxy tails (C<sub>1</sub> to C<sub>8</sub>, C<sub>10</sub>, C<sub>12</sub>, C<sub>14</sub>, C<sub>16</sub>, and C<sub>18</sub>) as well as halogen atoms (F, Cl, and Br) have been varied. The molecular structure of these compounds is shown in Scheme 1.

## 2. EXPERIMENTAL

### 2.1. General Information

All the solvents (acetone, methanol, ethanol, ethylacetate, and acetic acid) were obtained from local sources and purified as per the standard procedures. 4-Hydroxy-benzaldehyde,  $\alpha$ -naphthylamine, 4-fluoroaniline, 4-chloroaniline, 4-bromoaniline, and alkyl bromides were obtained from British Drug House, Poole, England and used without further purification. IR spectra were recorded using Elmer FTIR between 400–4000 cm<sup>-1</sup> spectral range. The UV/visible absorption spectra for the mesomorphic compounds were recorded in chloroform using a Shimadzu UV/PC 160-A spectrophotometer in the 200–800-nm spectral range. <sup>1</sup>H NMR spectra were recorded using a Jeol FX 300-MHz spectrometer, and the chemical shifts are reported in parts per million (ppm) relative to tetramethylsilane (TMS) as an internal standard. The purity of the compounds was checked by thin-layer chromatography and further confirmed by elemental analysis using a Coleman USA C, H, N analyser. The identification of the mesophases and the transition temperatures of the dimers were determined mainly by using a polarizing microscope (Leitz Labourlux) in conjunction with a programmable Kofler hot stage. For some representative compounds, transition temperatures and associated enthalpies were determined by differential scanning calorimetry using a DSC Mettler TA 4000 calorimeter at a rate of 10°C min<sup>-1</sup>.

## 2.2. Synthesis

### 2.2.1. 4-aminonaphthalene-1-haloazobenzene (4a-c)

These dyes were prepared [10–12] by condensing  $\alpha$ -naphthylamine with diazonium salts **5a–c** of substituted aniline (**6a–c**). First the substituted anilines **6a–c** were diazotised with dilute HCl and NaNO<sub>2</sub> at 0–5°C and coupled with  $\alpha$ -naphthylamine at pH 4–4.5. Then the reaction mixture was neutralized with dil. NaOH, and the obtained precipitate was collected by filtration and then air dried. The crude compounds were purified by repeated recrystallizations using abs. ethanol as solvent.

**4a**: A deep red crystalline solid; yield: 80%; mp: 151–152°C; elemental analysis calc. for C<sub>16</sub>H<sub>12</sub>N<sub>3</sub>F: C, 72.45; H, 4.52; N, 15.84; found: C, 72.43; H, 4.51; N, 15.82%.

**4b**: A deep red crystalline solid; yield: 85%; mp: 181–182°C; elemental analysis calc. for C<sub>16</sub>H<sub>12</sub>N<sub>3</sub>Cl: C, 68.2; H, 4.26; N, 14.92; found: C, 68.18; H, 4.24; N, 14.9%.

**4c**: A deep red crystalline solid; yield: 82%; mp: 176–177°C; elemental analysis calc. for C<sub>16</sub>H<sub>12</sub>N<sub>3</sub>Br: C, 58.89; H, 3.68; N, 12.88; found: C, 58.87; H, 3.66; N, 12.85%.

### 2.2.2. 4-n-alkoxybenzaldehydes (7a-m)

These were prepared by the reported method of Gray and Jones [13]. A mixture of 4-hydroxybenzaldehyde (1 mol) and K<sub>2</sub>CO<sub>3</sub> (1.5 mol) in 250 ml of anhyd. acetone was stirred and heated at 40°C while 1-bromoalkane (1.02 mol) was added slowly (1–2 h), after which mixture was refluxed for 16 h. The reaction mixture was cooled to room temperature and poured into water. The product obtained was extracted with ethyl ether several times, and the combine extracts were dried over MgSO<sub>4</sub> and concentrated at reduced pressure to obtain the crude product, which was purified as reported. The molecular structure of these aldehydes were confirmed by spectroscopic analyses and found to be in agreement with the reported data.

### 2.2.3. 4-[4'-n-alkoxybenzylideneamino]naphthalene-1-(4'-halo-1-azobenzene): (1a-m, 2a-m, and 3a-m)

To a stirred solution of the 4-aminonaphthalene-1-haloazobenzene (**4a–c**) (0.1 mol) in ethanol was added an appropriate alkoxyaldehyde (0.1 mol) and 2–3 drops of acetic acid [14]. The reaction mixture was reflux for 2–3 h. The orange precipitate was collected by filtration and washed with hot abs. ethanol. The crude products were recrystallized several times from ethyl acetate until constant transition temperatures were obtained. All the compounds were realized by this

method and exhibited spectral data consistent with their molecular structure. As representative cases we provide the molecular structural characterization data for **1d**, **2g**, and **3g**.

**1d**: An orange-red crystalline solid; mp 186–187°C; yield: 76%; UV-vis:  $\lambda_{\max} = 415.5 \text{ nm}$  ( $\epsilon = 1.3 \times 10^4 \text{ L mol}^{-1} \text{ cm}^{-1}$ ),  $268.4 \text{ nm}$  ( $\epsilon = 1.8 \times 10^4 \text{ L mol}^{-1} \text{ cm}^{-1}$ ); IR (KBr pellet):  $\nu_{\max}$  2881, 1630, 1602, 1417, 1366, 1261, 1170, 1070, 831, and  $720 \text{ cm}^{-1}$ ;  $^1\text{H NMR}$  ( $\text{CDCl}_3$ , 300 MHz):  $\delta$  8.97 (s, 1H,  $1 \times -\text{CH}=\text{N}-$ ), 8.4–7.1 (m, 14H, Ar), 4.05 (t, 2H,  $1 \times -\text{OCH}_2-$ ), 1.86–1.46 (m, 4H,  $2 \times -\text{CH}_2-$ ), and 1.03 (t, 3H,  $1 \times -\text{CH}_3$ ); elemental analysis calc. for  $\text{C}_{27}\text{H}_{24}\text{N}_3\text{O}$ : C, 76.23; H, 5.64; N, 9.88; found: C, 76.25; H, 5.68; N, 9.87%.

**2g**: An orange-red crystalline solid; mp 182–183°C; yield: 85%; UV-vis:  $\lambda_{\max} = 423 \text{ nm}$  ( $\epsilon = 0.65 \times 10^4 \text{ L mol}^{-1} \text{ cm}^{-1}$ ),  $273.8 \text{ nm}$  ( $\epsilon = 1.35 \times 10^4 \text{ L mol}^{-1} \text{ cm}^{-1}$ ); IR (KBr pellet):  $\nu_{\max}$  2868, 1629, 1602, 1430, 1378, 1240, 1163, 1056, 834, and  $722 \text{ cm}^{-1}$ ;  $^1\text{H NMR}$  ( $\text{CDCl}_3$ , 300 MHz):  $\delta$  8.97 (s, 1H,  $1 \times -\text{CH}=\text{N}-$ ), 8.43–7.1 (m, 14H, Ar), 4.05 (t, 2H,  $1 \times -\text{OCH}_2-$ ), 1.86–1.46 (m, 10H,  $5 \times -\text{CH}_2-$ ), and 0.91 (t, 3H,  $1 \times -\text{CH}_3$ ); elemental analysis calc. for  $\text{C}_{30}\text{H}_{30}\text{N}_3\text{OCl}$ : C, 74.45; H, 6.2; N, 8.68; found: C, 74.5; H, 6.15; N, 8.66%.

**3g**: An orange-red crystalline solid; mp 178–179°C; yield: 82%; UV-vis:  $\lambda_{\max} = 424 \text{ nm}$  ( $\epsilon = 1.6 \times 10^4 \text{ L mol}^{-1} \text{ cm}^{-1}$ ),  $269.4 \text{ nm}$  ( $\epsilon = 1.3 \times 10^4 \text{ L mol}^{-1} \text{ cm}^{-1}$ ); IR (KBr pellet):  $\nu_{\max}$  2868, 1630, 1602, 1423, 1373, 1252, 1163, 1064, 834, and  $720 \text{ cm}^{-1}$ ;  $^1\text{H NMR}$  ( $\text{CDCl}_3$ , 300 MHz):  $\delta$  8.97 (s, 1H,  $1 \times -\text{CH}=\text{N}-$ ), 8.43–7 (m, 14H, Ar), 4.05 (t, 2H,  $1 \times -\text{OCH}_2-$ ), 1.86–1.44 (m, 10H,  $5 \times -\text{CH}_2-$ ) and 0.91 (t, 3H,  $1 \times -\text{CH}_3$ ); elemental analysis calc. for  $\text{C}_{30}\text{H}_{30}\text{N}_3\text{OBr}$ : C, 68.18; H, 5.68; N, 7.95; found: C, 68.15; H, 5.66; N, 7.93%.

## 3. RESULTS AND DISCUSSION

### 3.1. Synthesis

The target molecules of the three series **1a–m**, **2a–m**, and **3a–m**, and their intermediates **4a–c**, **5a–c**, and **7a–m** were synthesized as outlined in Scheme 1. The requisite 4-*n*-alkoxybenzaldehydes (**7a–m**) were prepared by refluxing 4-hydroxybenzaldehyde with 1-*n*-bromoalkane under mild basic reaction conditions in a solvent medium [13]. The key intermediates, azonaphthylene amines **4a–c**, were realized by coupling  $\alpha$ -naphthylamine with diazonium salts **5a–c**, which in turn were prepared by the diazotization of 4-haloanilines (**6a–c**). Finally, the aldehydes **7a–m** were condensed with azonaphthylene amines **4a–c** under mild acidic reaction conditions in ethanol to obtain the target molecules in reasonably good yields. The molecular

structures of all the compounds were confirmed by spectroscopic analysis (see Experimental section).

### 3.2. Thermal Behavior

As mentioned earlier, in an effort to understand the structure–property relation, the chain length of the terminal alkoxy tail as well as the terminal halogen substitutions have been varied, which resulted in three series of compounds, series 1 (**1a–m**), series 2 (**2a–m**), and series 3 (**3a–m**). The transition temperatures and the phase sequence of the compounds synthesized in the present investigation are presented in Tables 1, 2, and 3. The mesomorphic behavior of the target compounds have been evaluated by optical studies. However, for some representative compounds, the phase transition temperatures have been confirmed by calorimetric studies, which are presented in Table 4. All the members of the three series exhibit nematic (N) and/or smectic A (SmA) phases. The nematic phase was identified based on the observation of a characteristic schlieren (Fig. 1) or marble texture when unrubbed slides treated for planar orientation were used. In a homeotropically aligned sample, the N phase shows a pseudoisotropic texture, which flashed when subjected to shearing stress. The presence

**TABLE 1** Transition Temperatures (°C) of Compounds<sup>a</sup> of Series 1

Compounds		Transition temperatures						
No.	R	Cr	Heating	SmA	Heating	N	Heating	I
<b>1a</b>	CH <sub>3</sub>	•	150	-		•	194	•
<b>1b</b>	C <sub>2</sub> H <sub>5</sub>	•	152	-		•	203	•
<b>1c</b>	C <sub>3</sub> H <sub>7</sub>	•	140	-		•	189	•
<b>1d</b>	C <sub>4</sub> H <sub>9</sub>	•	146	-		•	186	•
<b>1e</b>	C <sub>5</sub> H <sub>11</sub>	•	133	-		•	172	•
<b>1f</b>	C <sub>6</sub> H <sub>13</sub>	•	119	-		•	169	•
<b>1g</b>	C <sub>7</sub> H <sub>15</sub>	•	112	-		•	162	•
<b>1h</b>	C <sub>8</sub> H <sub>17</sub>	•	99	-		•	156	•
<b>1i</b>	C <sub>10</sub> H <sub>21</sub>	•	112	-		•	147	•
<b>1j</b>	C <sub>12</sub> H <sub>25</sub>	•	89	•	(57) <sup>b</sup>	•	132	•
<b>1k</b>	C <sub>14</sub> H <sub>29</sub>	•	95	•	101	•	135	•
<b>1l</b>	C <sub>16</sub> H <sub>33</sub>	•	91	•	109	•	128	•
<b>1m</b>	C <sub>18</sub> H <sub>37</sub>	•	90	•	112	•	123	•

<sup>a</sup>Temperatures ascertained by optical microscopic observation at a rate of 3°C/ min.

<sup>b</sup>Monotropic transition.

• = phase exists; - = phase does not exist.

Cr = crystal; SmA = smectic A; N = nematic phase; I = isotropic phase.

**TABLE 2** Transition Temperatures ( $^{\circ}\text{C}$ ) of Compounds<sup>a</sup> of Series 2

Compounds		Transition temperatures						
No.	R	Cr	Heating	SmA	Heating	N	Heating	I
<b>2a</b>	CH <sub>3</sub>	•	170	-		•	234	•
<b>2b</b>	C <sub>2</sub> H <sub>5</sub>	•	155	-		•	238	•
<b>2c</b>	C <sub>3</sub> H <sub>7</sub>	•	139			•	224	•
<b>2d</b>	C <sub>4</sub> H <sub>9</sub>	•	132			•	209	•
<b>2e</b>	C <sub>5</sub> H <sub>11</sub>	•	120			•	195	•
<b>2f</b>	C <sub>6</sub> H <sub>13</sub>	•	127			•	185	•
<b>2g</b>	C <sub>7</sub> H <sub>15</sub>	•	114			•	182	•
<b>2h</b>	C <sub>8</sub> H <sub>17</sub>	•	122			•	179	•
<b>2i</b>	C <sub>10</sub> H <sub>21</sub>	•	112	•	(83) <sup>b</sup>	•	168	•
<b>2j</b>	C <sub>12</sub> H <sub>25</sub>	•	101	•	109	•	160	•
<b>2k</b>	C <sub>14</sub> H <sub>29</sub>	•	90	•	120	•	151	•
<b>2l</b>	C <sub>16</sub> H <sub>33</sub>	•	82	•	128	•	149	•
<b>2m</b>	C <sub>18</sub> H <sub>37</sub>	•	87	•	122	•	135	•

<sup>a</sup>Temperatures ascertained by optical microscopic observation at a rate of 3 $^{\circ}\text{C}/\text{min}$ .

<sup>b</sup>Monotropic transition.

of the SmA phase has been confirmed based on the microscopic observation of the characteristic focal-conic texture (Fig. 2) in slides treated for planar orientation and a dark field of view in slides treated for

**TABLE 3** Transition Temperatures ( $^{\circ}\text{C}$ ) of Compounds<sup>a</sup> of Series 3

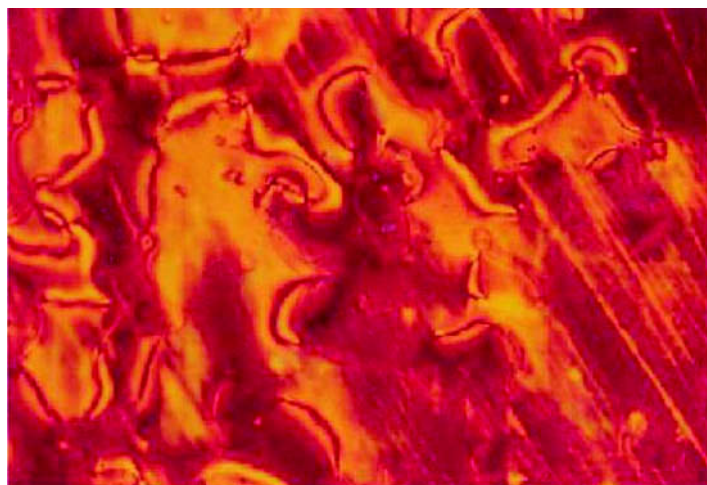
Compounds		Transition temperatures						
No.	R	Cr	Heating	SmA	Heating	N	Heating	I
<b>3a</b>	CH <sub>3</sub>	•	183	-		•	236	•
<b>3b</b>	C <sub>2</sub> H <sub>5</sub>	•	168	-		•	248	•
<b>3c</b>	C <sub>3</sub> H <sub>7</sub>	•	142			•	229	•
<b>3d</b>	C <sub>4</sub> H <sub>9</sub>	•	129			•	212	•
<b>3e</b>	C <sub>5</sub> H <sub>11</sub>	•	130			•	192	•
<b>3f</b>	C <sub>6</sub> H <sub>13</sub>	•	122			•	186	•
<b>3g</b>	C <sub>7</sub> H <sub>15</sub>	•	125			•	179	•
<b>3h</b>	C <sub>8</sub> H <sub>17</sub>	•	130			•	175	•
<b>3i</b>	C <sub>10</sub> H <sub>21</sub>	•	115	•	(85) <sup>b</sup>	•	166	•
<b>3j</b>	C <sub>12</sub> H <sub>25</sub>	•	102	•	109	•	161	•
<b>3k</b>	C <sub>14</sub> H <sub>29</sub>	•	97	•	119	•	153	•
<b>3l</b>	C <sub>16</sub> H <sub>33</sub>	•	80	•	131	•	150	•
<b>3m</b>	C <sub>18</sub> H <sub>37</sub>	•	88	•	120	•	137	•

<sup>a</sup>Temperatures ascertained by optical microscopic observation at a rate of 3 $^{\circ}\text{C}/\text{min}$ .

<sup>b</sup>Monotropic transition.

**TABLE 4** DSC Data for Some Representative Compounds of Series 1, 2, and 3

Compound	Transition	Peak temp °C (microscopic temp.)	$\Delta H/Jg^{-1}$	$\Delta S/Jg^{-1}k^{-1}$	Total entropy change $\Delta S/Jg^{-1}k^{-1}$
<b>1d</b>	Cr $\rightarrow$ N	143.4 (146)	212.3	1.48	1.5
	N $\rightarrow$ I	185.8 (186)	3.5	0.019	
<b>1m</b>	K $\rightarrow$ SmA	90.7 (91)	112.1	1.2358	1.25
	SmA $\rightarrow$ N	— (109)	—	—	
<b>2g</b>	N $\rightarrow$ I	127.8 (128)	1.18	0.013	1.42
	K $\rightarrow$ N	115.4 (114)	162.4	1.48	
<b>2j</b>	N $\rightarrow$ I	181.3 (182)	1.65	0.0091	4.29
	K $\rightarrow$ SmA	101.44 (101)	431.9	4.26	
<b>3i</b>	SmA $\rightarrow$ N	— (109)	—	—	5.39
	N $\rightarrow$ I	159.6 (160)	5.508	0.035	
<b>3m</b>	K $\rightarrow$ N	116.3 (115)	622.1	5.3482	2.11
	N $\rightarrow$ I	164.53 (166)	6.429	0.039	
<b>3m</b>	K $\rightarrow$ SmA	91.33 (88)	189.1	2.0705	5.856
	SmA $\rightarrow$ N	— (120)	—	—	
	N $\rightarrow$ I	137.0 (137)	5.856	0.043	

**FIGURE 1** Photomicrograph of a characteristic schlieren texture of the nematic phase observed for the compound **3i** at 159°C while cooling the sample from the isotropic phase.

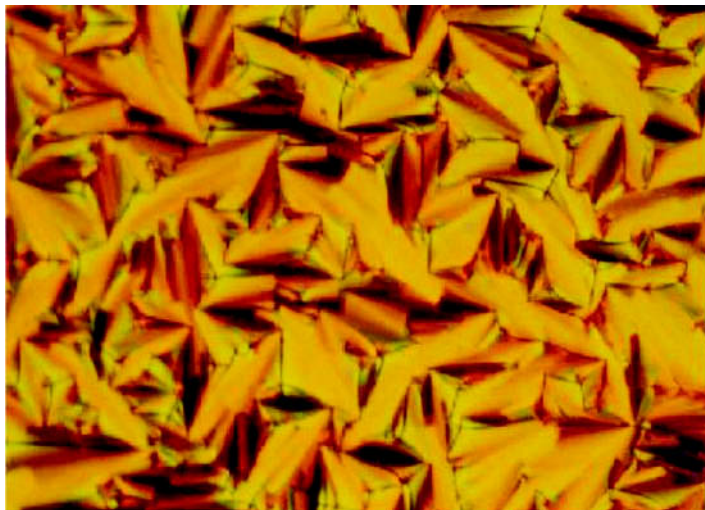


**FIGURE 2** Photomicrograph of the characteristic focal-conic texture seen in slides treated for planar orientation of the compound **11** at 105°C while cooling from the isotropic phase.

homeotropic orientation. When untreated slides were employed, both the focal-conic and psuedoisotropic textures have been observed. As can be seen in Table 1, fluoro-substituted compounds with  $C_1$  to  $C_{10}$  tail display an enantiotropic N phase, whereas the compound with the  $C_{12}$  tail also shows the monotropic SmA phase. The higher homologues with  $C_{14}$ ,  $C_{16}$ , and  $C_{18}$  tails exhibit both enantiotropic SmA and N phases. The dependence of the transition temperatures on the number of carbon atoms in the alkoxy chain of this series has been shown in Fig. 3. As the chain length increases, the terminal cohesive forces, which account for nematic–isotropic change, decrease, as result of which the nematic–isotropic curve obtained for even members in these series is falling one. A similar curve should be obtained for odd members, but in practice a rising curve is obtained, which shows a falling tendency from the middle member. This may probably due to relative differences between the terminal and lateral cohesions. As the chain length increases, lateral cohesion increases and it may support the terminal forces; this, to a certain degree, helps in explaining the rise in the curve, which afterward shows the tendency of becoming a normal falling curve. Probably these differences may be due to differences in packing and cohesion between the terminal methyl groups of alkoxy chains containing odd and even numbers of carbon atoms.

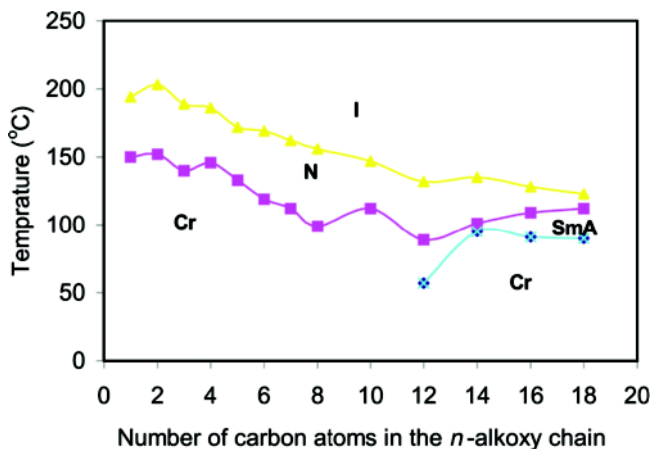


**FIGURE 3** Plot of transition temperature against the number of carbon atoms in the *n*-alkoxy chains for the compounds of series 1.

Thermal behavior of the compounds with chloro (Table 2) and bromo (Table 3) substitutions (series 2 and series 3) is almost similar to that of compounds of series 1. The dependence of the transition temperatures on the number of carbon atoms in the alkoxy chain of series

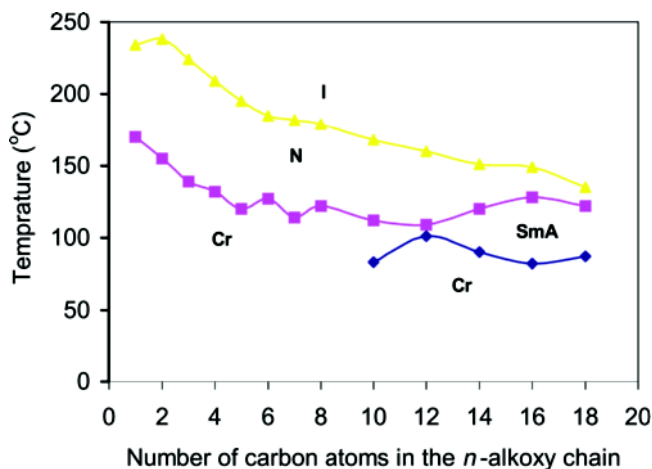


**FIGURE 4** Plot showing the dependence of transition temperature against the number of carbon atoms in the *n*-alkoxy chains for the chloro compounds of series 2.

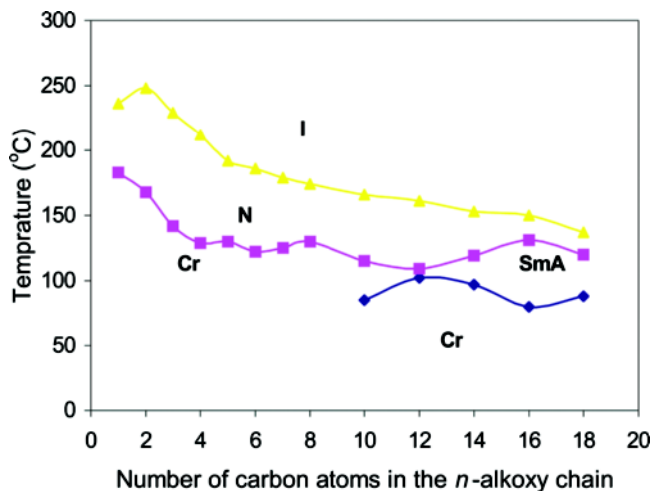


**FIGURE 5** Plot of transition temperature against the number of carbon atoms in the *n*-alkoxy chains for the compounds of series 3.

2 and series 3 shown in Figs. 4 and 5 respectively. The smectic phase begins to appear from  $C_{10}$  derivatives in both the cases, which perhaps could be attributed to the fact that the overall polarizability of the chloro- and bromo-substituents is higher than that of the fluoro-substituent. Further, the transition temperatures, in particular the N-Iso, is lower for compounds with fluoro-substitution, which is attributed to low polarity and low intermolecular attractive forces of these molecules.

#### 4. SUMMARY

In conclusion we have synthesized as many as 39 new naphthalene core-based mesogens with azo linkage and evaluated their mesomorphic behavior. These compounds form three series of compounds resulting from the variations in two terminal substitutions. To understand structure–property relations alkoxy tails ( $C_1$  to  $C_8$ ,  $C_{10}$ ,  $C_{12}$ ,  $C_{14}$ ,  $C_{16}$ , and  $C_{18}$ ) and halogen atoms (F, Cl, and Br) as terminal substituents have been varied. Our investigations reveal that, in general, all the compounds display nematic and or smectic A mesophases. The lower and middle homologues exhibit the nematic phase only whereas higher homologues also display the smectic A phase. Thus, the thermal behavior of these compounds is reminiscent of a large number of homologues series reported in the literature.

## REFERENCES

- [1] Castellano, J. A. (1972). *RCA. Rev.*, 33, 296.
- [2] Gray, G. W. (1962). *Molecular structure and properties of liquid crystal*, Academic Press: New York.
- [3] Billard, J., Dubois, J. S., & Zaon, A. (1975). *J. Phys. (Paris), Colloq.*, C1, 355.
- [4] Wiegand, C. Z. (1954). *Naturforsch.*, 9b, 516.
- [5] Wiegand, C. Z. (1941). *Hand-und Jahrbuch Der Chem. Physik*, Vol. 2; Chap, C., Akad. Verl. (Leipzig); (1943). *Chem. Abstr.*, 37, 1078.
- [6] Dave, J. S., Kurian, G., Prajapati, A. P., & Vora, R. A. (1971). *Mol. Cryst. Liq. Cryst.*, 14, 307.
- [7] Dave, J. S., Kurian, G., Prajapati, A. P., & Vora, R. A. (1972). *Curr. Sci.*, 41, 415.
- [8] Dave, J. S., Kurian, G., Prajapati, A. P., & Vora, R. A. (1972). *Indian J. Chem.*, 10, 754.
- [9] Arora, S. L. & Ferguson, J. L. (1971). *Simp. Faraday Soc Liquid Crystals*, 5, 97.
- [10] Keller, P. & Libert, L. (1978). *Solid St. Phys. Suppl.*, 14, 19.
- [11] Karaer, H. (1997). Doctoral thesis, Ondokur Mayıs University, Institute of Natural and Applied Science, Dept. of Chemistry.
- [12] Tandel, R. S. (2000). Ph. D. thesis, Dept. of Chemistry, South Gujarat University.
- [13] Gray, G. W. & Jones, B. (1954). *J. Chem. Soc.*, 1467.
- [14] Schiff, H. (1864). *Ann.*, 131, 188.